

FeatFSDA: Towards Few-shot Domain Adaptation for Video-based Activity Recognition

Kunyu Peng¹, Di Wen¹, David Schneider¹, Jiaming Zhang¹, Kailun Yang^{2,*},
M. Saquib Sarfraz¹, Rainer Stiefelhagen¹, Alina Roitberg¹
¹Karlsruhe Institute of Technology, ²Hunan University

ABSTRACT

Domain adaptation is essential for activity recognition, as common spatiotemporal architectures risk overfitting due to increased parameters arising from the temporal dimension.

Unsupervised domain adaptation methods have been extensively studied, yet, they require large-scale unlabeled data from the target domain. In this work, we address *few-shot domain adaptation for video-based activity recognition (FSDA-AR)*, which leverages a very small amount of labeled target videos to achieve effective adaptation. This setting is attractive and promising for applications, as it requires recording and labeling only a few, or even a single example per class in the target domain, which often includes activities that are rare yet crucial to recognize. We construct FSDA-AR benchmarks using five established datasets: UCF101, HMDB51, EPIC-KITCHEN, Sims4Action, and Toyota Smart Home. Our results demonstrate that FSDA-AR performs comparably to unsupervised domain adaptation with significantly fewer (yet labeled) target examples. We further propose a novel approach, FeatFSDA, to better leverage the few labeled target domain samples as knowledge guidance. FeatFSDA incorporates a latent space semantic adjacency loss, a domain prototypical similarity loss, and a graph-attentive-network-based edge dropout technique. Our approach achieves state-of-the-art performance on all datasets within our FSDA-AR benchmark. To encourage future research of few-shot domain adaptation for video-based activity recognition, we will release our benchmarks and code at [FeatFSDA](#).

CCS CONCEPTS

• **Computing methodologies** → **Activity recognition and understanding**; **Supervised learning by classification**.

KEYWORDS

Domain adaptation, video-based activity recognition

1 INTRODUCTION

Domain shifts (distribution discrepancies between the source domain training data and the target test data) are inevitable in real-world applications, and the performance of human activity recognition models is strongly affected by, *e.g.*, changes in sensor types and placements, room layouts or transitions from synthetic to real examples [12, 48]. The vast majority of the existing Domain Adaptation (DA) research concentrates on the Unsupervised Domain Adaptation (UDA) [7–9, 19, 29, 49, 62, 67], and Semi-supervised Domain Adaptation (SSDA) settings [34, 50, 69, 70]. These paradigms allow us to transfer the recognition ability from the source domain to the target domain. The benefit of DA lies in its reduction of labor-intensive

*Corresponding author (e-mail: kailun.yang@hnu.edu.cn).

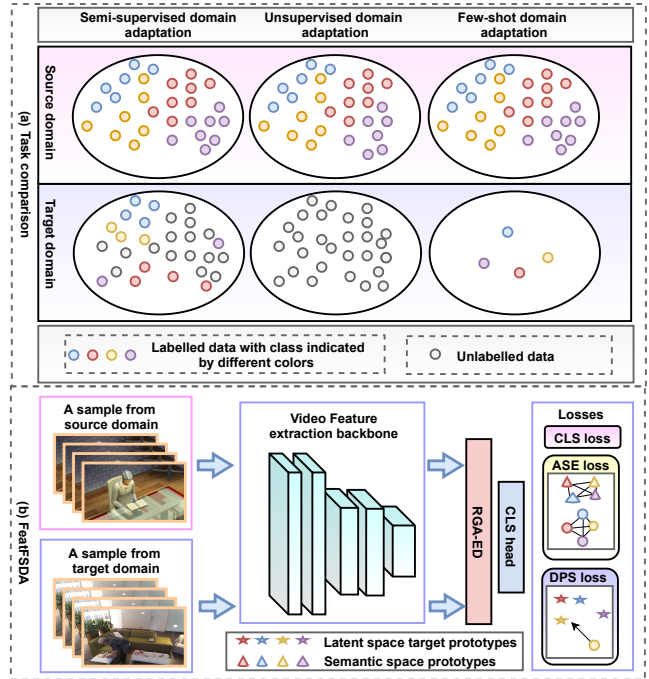


Figure 1: (a) A comparison of the semi-supervised domain adaptation (SSDA), unsupervised domain adaptation (UDA), and few-shot domain adaptation (FSDA) tasks. (b) An overview of our proposed FeatFSDA pipeline.

labeling tasks for large-scale data in the target domain. However, as shown in Figure 1(a), UDA and SSDA paradigms both require a substantial amount of samples from the target domain, while SSDA further demands a few labels from the target domain.

To address this drawback, we take a step towards the relatively uncharted area of **Few-Shot Domain Adaptation for Action Recognition (FSDA-AR)** illustrated in Figure 1(a). Instead of relying on a large number of examples from the target domain, FSDA-AR necessitates a minimal amount of labeled samples, *e.g.*, requiring only a few or even a single annotated sample per class in the target domain. These labeled target domain samples serve as knowledge support to reduce the domain gap. Unlike pixel-wisely annotated tasks such as semantic segmentation [17], human activity recognition only requires a single label assigned to a video snippet. Consequently, annotating a few target samples for the FSDA-AR task is less time-consuming and therefore more feasible. Despite this advantage, little research was performed on FSDA-AR, so far. Of the two published works most related to our tasks, one targets FSDA-AR in videos but the benchmark is not made available [20], while another work [38]

tackles only a specific data type (radar-based activity recognition) that is not well-suited for general activity recognition.

To delve deeper into FSDA-AR for human activity recognition, we adopt the evaluation procedure of five public video-based human activity recognition datasets to our task. To study FSDA-AR in diverse settings featuring small and large domain gaps, we consider Sims4Action [48] → Toyota Smart Home (TSH) [13], EPIC-KITCHEN-55 [12], HMDB [32] → UCF [53], and UCF [53] → HMDB [32]. This benchmark selection covers a transfer between real-world activity recognition datasets with similar perspectives (small domain gap), adaptation towards the egocentric camera view domain, and adaptation from synthesized to real-world data (large domain gap). In this benchmark, we include various approaches as baselines, such as UDA approaches reformulated into the FSDA-AR setting and statistical methods.

We also propose a new approach for better few-shot domain adaptation in the video, which we refer to as FeatFSDA (an overview is provided in Figure 1(b)). Our design choices are driven by (1) enhancing the generalization of *temporal* data, (2) learning a joint embedding space of both domains and (3) effectively leveraging the few labeled target-domain samples. First, the RNN-based Graph Attentive Video Clip Aggregation mechanism with Edge Dropout (RGA-ED) is employed, as our data inherently has a temporal component. This mechanism enhances the generalizability of temporal aggregation by leveraging a graph neural network (GNN), while random edge dropout serves as an additional regulariser to improve domain generalization. Second, the Semantic Embedding treats the few labeled target examples as graph nodes. This graph is based on BERT-derived features and aligns distance-based Adjacency graphs of Semantic Embeddings (ASE) from the video latent space with the corresponding semantic latent space, therefore aligning the domains. Finally, the Domain Prototypical Similarity (DPS) loss ensures that the source latent space embeddings are similar to the corresponding class prototypes obtained from the few labeled target domain samples.

FeatFSDA yields state-of-the-art performance on all datasets considered in our FSDA-AR benchmark.

Our contributions can be summarized as follows:

- We explore the under-researched task of Few-Shot Domain Adaptation for Activity Recognition (FSDA-AR) by formalizing new evaluation protocols on five established datasets with different domain shifts, including third-person and egocentric perspectives as well as synthetic and real data.
- We propose the new FeatFSDA approach, consisting of three key components: RNN-based Graph Attentive Video Clip Aggregation (RGA-ED) for temporal generalizability of video data, an Alignment-aware Semantic Embedding (ASE) graph for bridging source and target domains, and the Domain Prototypical Similarity (DPS) loss function for effective utilization of labeled target domain samples.
- Our approach achieves state-of-the-art results on the FSDA-AR benchmark considering the 1-, 5-, 10-, 20-shot settings. Compared with the UDA task, the approaches under the FSDA-AR task reach comparable performance to the approaches under the UDA task on most of the used datasets. Especially on the UCF → HMDB, 5-shot, FeatFSDA could

achieve 90.3% Top-1 accuracy which is much higher than that of the state-of-the-art approach of the UDA task.

2 RELATED WORK

In this section, we will give an overview of the related works considering two major areas: domain adaptation and activity recognition.

Domain Adaptation (DA). Domain adaptation (DA) [4, 5, 7, 8, 11, 20, 21, 26, 27, 29, 36–38, 40, 42, 45, 49, 50, 62, 64, 65, 68, 71] refers to a situation in which training and test data come from two domains that are related, but distinct from one another. Adapting a learner to a target domain is the goal of DA. Unsupervised domain adaptation (UDA) aims to solve this problem of inter-domain discrepancy without labeling target domain samples in training. Image-based tasks have been widely proposed using UDA methods [4, 6, 15, 29, 33, 36, 40, 54, 65]. DAN [40] and JAN [41] proposed to align the marginal distributions of the source and target domains in the feature space by minimizing maximum mean discrepancy (MMD) and joint maximum mean discrepancy (JMMD), respectively. For the video-based UDA, several existing works use an adversarial learning framework to deal with the domain shifts [7, 8, 11] while Wei *et al.* [62] use disentanglement learning. CoMix [49] uses mixture techniques to better leverage the background information from the target domain. The semi-supervised domain adaptation (SSDA) [34, 35, 47, 50, 69, 70] relaxes the strict constraint of UDA by using a partially annotated target set.

In few shot domain adaptation (FSDA) [24, 28, 43, 56, 68], only a few labeled samples per class are given to formulate the target domain training set. Note that FSDA-AR does not rely on a large-scale unlabeled training set from the target domain to achieve the DA for human activity recognition while SSDA needs a large amount of the unlabeled data from target domain. Yet, the research of FSDA for video-based activity recognition (FSDA-AR) has been very limited with only two published works targeting this task [20, 38]. PASTN [20] uses an attentive adversarial network to learn domain-invariant features. FS-ADA [38] integrates both the category classifier and the domain discriminator to extract domain-invariant and category-discriminative features. However, since the benchmark of PASTN [20] is not available and FS-ADA [38] uses radar data, there is a strong need for further research of video-based FSDA-AR, which is the main motivation of our work. We, therefore, introduce the first publicly available video-based FSDA-AR benchmark and consider diverse domain combinations. We further propose the FeatFSDA approach, which uses three key components to increase the generalization of video data: an RNN-based graph attentive network with edge dropout to improve the generalization considering the *temporal* aggregation, a joint semantic embedding space, as well as the domain prototypical similarity loss to better utilize the few labeled examples existing in the target domain.

Video-based Human Activity Recognition (HAR). Supervised human activity recognition methods [2, 3, 18, 25, 46, 52, 57, 61, 63, 66, 73] have achieved impressive results with deep learning algorithms in recent years. The video-based approaches can be grouped into convolutional neural network-based (CNN) and transformer-based methods. For CNN-based methods, most of the existing approaches leverage 3D CNN and diverse temporal aggregation techniques. TSN [61] samples a fixed number of video frames evenly

across the video segments, and use these sampled frames as input for a two-stream network. I3D [3] uses an inflated Inception v1 model [55] with 3D convolutional layers utilized in each stage. S3D [66] decomposes the lower 3D convolutional layers of I3D into two separate operations, a spatial and temporal convolution. X3D [18] expands a tiny base 2D image architecture into a spatiotemporal one by expanding multiple possible axes in space, time, channels, and depth. As a result, an optimal trade-off is achieved between accuracy and complexity. Another group of network architectures leverages Transformer-based backbones [1, 16, 39]. Most of existing UDA works [7, 8, 11, 49, 62] make use of I3D [3] or ResNet [22] as the feature extractor. Following the standard setting of UDA [7, 8, 11, 49, 62], we also leverage I3D [3] as our backbone in the proposed FeatFSDA method, allowing adequate comparison between the FSDA-AR and UDA tasks.

3 METHODOLOGY

3.1 Problem formulation

Comparison with other domain adaptation settings. We begin by distinguishing the task we address from the domain adaptation settings commonly used in previous research. The task we address is Few-Shot Domain Adaptation (FSDA), where a very small amount of labeled examples are available for each category in the target domain. The comparison among the commonly addressed tasks of Semi-Supervised Domain Adaptation (SSDA) [34, 50, 69, 70], Un-supervised Domain Adaptation (UDA) [7–9, 19, 29, 49, 62, 67], and our FSDA is provided in Figure 1. In contrast to FSDA, both UDA and SSDA necessitate a large amount of unlabeled data in the target domain, and collecting such large-scale data might be not feasible in certain applications. FSDA, on the other hand, requires only a small number of labeled examples from the target domain, balancing the trade-off between data collection expenses and labeling efforts. In our FSDA-AR benchmark, the leveraged few shot setting results in a 70%to98% reduction in terms of the amount of data required by the target domain compared to SSDA and UDA. Activity recognition does not rely on pixel-level dense annotation, which makes the trade-off between annotation and data collection considerable. It is crucial to note that FSDA is distinct from domain adaptation for few-shot learning [10, 72], which is specifically designed for adapting to new classes with limited examples, while we are adapting to new domains. FSDA does not encompass new activity classes.

FSDA formulation. The task we address assumes a fully labeled large-scale source domain training set $D_s = (v_i^s, l_i^s)_{i=1}^{N_s^{train}}$ and a small target domain training set $D_t = (v_i^t, l_i^t)_{i=1}^{N_t^{train}}$, which contains only a few labeled samples per class. Our objective is to train a model using both D_s and D_t so that the resulting model performs well on the target domain test set, denoted as $T_t = (v_i^t, l_i^t)_{i=1}^{N_t^{test}}$. In this context, N_s^{train} , N_t^{train} , and N_t^{test} represent the number of samples in the source domain training set, target domain training set, and target domain test set, respectively. The index of the sample is represented by i , while the video samples and corresponding labels are represented by v and l . The source and target domains are denoted by s and t , respectively.

3.2 Baselines on FSDA-AR benchmark

We construct challenging baselines for our FSDA-AR benchmark by using two FSDA-AR approaches, FS-ADA [38] and PASTN [20], established UDA approaches, *e.g.*, TA³N [7, 8], TranSVAE [62] reformulated for our task, CoMix [49], and CO²A [11], as well as the statistical baselines random chance, K-nearest neighbors (KNN) and Nearest Center. For consistency, we use the I3D-backbone [3] pre-trained on Kinetics400 [30] for all baselines.

Statistical baselines. We first use the I3D backbone [3] pre-trained on Kinetics400 [30] to extract video features, discarding the last classification layer. All the statistical baselines (except for the Random baseline) are based on the extracted features. For the Random method, we randomly assign a class to a test set sample to establish the lower bound. In the KNN method, we assign a label to a test set sample by averaging the performance of the 3-, 5- and 10-NN methods, with neighbors selected from the source domain training set. For the Nearest Center method, we first calculate class centers in the source domain training set and then assign the label of the nearest class center in the source domain to the target domain test set sample. In the Nearest Neighbor method, we assign the label of the nearest sample in the source domain training set to the query samples from the target domain test set. Since these statistical baselines use the same source domain training set as support, the performance keeps the same across different shot settings. These statistical baselines are used to showcase the domain generalization (DG) performance when no few shot sample from the target domain is provided to better illustrate the benefits brought by the provided few shot samples through the comparison with FSDA approaches.

Unsupervised domain adaptation (UDA) baselines. To enrich our FSDA-AR benchmark and enable comparisons with the existing Domain Adaptation (DA) frameworks, we implement and restructure several established video-based UDA methods to suit the FSDA-AR task. This is achieved by incorporating supervised classification loss on samples from the target domain training set and converting the unsupervised contrastive loss into triplet margin loss. Specifically, we leverage four prominent methods: TA³N [7, 8], TranSVAE [62], CO²A [11] and CoMix [49], where TA³N and CO²A leverage domain adversarial learning, TranSVAE concentrates on domain disentanglement and CoMix targets mixture techniques.

Few-shot domain adaptation (FSDA) baselines. We employ two existing approaches for FSDA-AR. The first is FS-ADA [38], which targets radar-based FSDA using adversarial domain adaptation. The second is PASTN [20], which introduces a pairwise attentive adversarial spatiotemporal network. As the benchmarks and code for both methods are unavailable, we first create a new benchmark using publicly accessible datasets and then replicate their performance on our FSDA-AR benchmark.

3.3 FeatFSDA

In this section, we present the key components of our proposed FeatFSDA approach (depicted in Figure 2), which is designed for the FSDA-AR task. FeatFSDA incorporates a semantic adjacency loss (ASE loss), a prototypical similarity loss (DPS loss), and a graph attentive network-based edge dropout technique (RGA-ED) while utilizing I3D [3] to extract clip-wise features. This ensures a fair comparison with UDA methods, as most of them employ I3D as

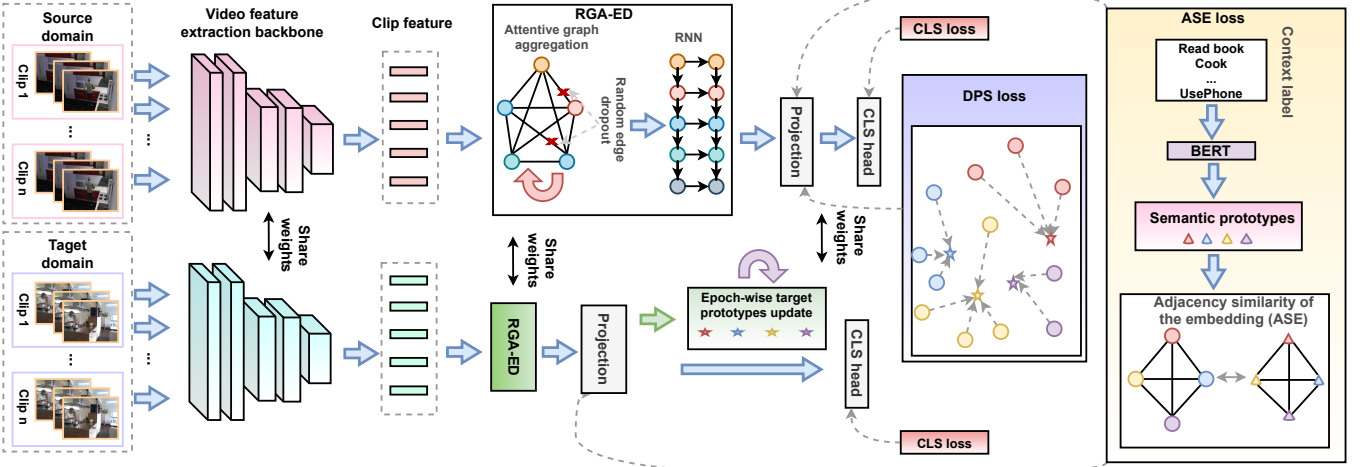


Figure 2: An overview of the proposed FeatFSDA. The input video is first separated into overlapped clips extracted through a fixed-size sliding window and then fed into the video feature extraction backbone to extract clip-level features. Then, RGA-ED is used for clip aggregation considering both domains, where the edge dropout is leveraged only in training to introduce more generalizability to the model. A domain prototypical similarity (DPS) loss and an adjacency similarity (ASE) loss, where the semantic embedding space calculated through the context description of the labels is used, and a classification loss is leveraged for the supervision.

their backbone. In the following subsections, we will discuss each component in greater detail.

Clip-wise video feature extraction. Similarly to our baselines, we adopt I3D [3] as our backbone for computing video representations and temporal sliding windows to extract the clip feature for a given video. Let us consider a video sample represented as $v = \{v_0, \dots, v_{N_T-1}\}$, where v_i indicates the i -th frame of the given video v , N_w is the window size of the sliding window and N_T is the number of the frames. We can then obtain a set of video clips, denoted as $Set\{\hat{v}_i\} = \{\{v_i, \dots, v_{i+N_w}\} \mid i \in [0, N_T - 1]\}$ (zero padding is used at the start and end of the video). Next, we extract clip-level features for all the videos. By inputting these clips into the previously mentioned I3D-based feature extractor H_α , we can acquire the set of clip features as $Set\{f_i\} = \{H_\alpha(\hat{v}_i) \mid i \in [0, N_T - 1]\}$.

RGA-ED temporal aggregation mechanism. Since human activity recognition models inherently operate on *sequences* with causal connections between the observed states in the individual frames, our first idea is to explicitly tackle temporal generalization. After the acquisition of the clip-level feature for one given video, we propose to leverage a new RNN-based graph attentive aggregation mechanism with edge dropout (RGA-ED) to improve model versatility in terms of temporal causal aggregation. Each clip is regarded as a node to construct the temporal causal graph structure. With F denoting $Set\{f_i\}$, we first construct a fully-connected graph, where each clip is connected to the following clips according to the temporal causal order. Assuming the edge connection is denoted by a binary matrix as $Q = \{q_{(i,j)}\}$ with $q_{(i,j)}$ as the directional connection indicator between the clips i and j , where $q_{(i,j)}$ are calculated as:

$$Q = \{q_{(i,j)} \mid i \in [0, N_s - 1], j \in [0, N_s - 1]\},$$

$$\text{where } q_{(i,j)} = \begin{cases} 1, & j > i \\ 0, & i > j. \end{cases} \quad (1)$$

During training, the edges are randomly discarded with a ratio μ to introduce temporal-level uncertainty and to improve the cross-domain generalization of the temporal aggregation network. Thereby, the edges used in training are Q^* , which is calculated through Eq. 2:

$$Q^* = \text{RandomSelect}_\mu\{Q\}. \quad (2)$$

We then build up graph attentive architecture using the scheme of [?] together with the aforementioned temporal causal graph to achieve the further aggregation of the clip features. The attentive value of each node is calculated as:

$$r_{(i,j)} = \frac{\exp(\sigma(P_\beta(\text{Cat}(P_Y(f_i), P_Y(f_j))))))}{\sum_{k \in [0, N_s-1]} (\exp(\sigma(P_\beta(\text{Cat}(P_Y(f_i), P_Y(f_k))))))}, \quad (3)$$

where $r_{(i,j)}$ indicates the clip importance; σ denotes the non-linear activation, *i.e.*, LeakyReLU; P_Y and P_β denote linear projections. Cat indicates the concatenation of the derived linear projected features from different nodes. N_s indicates the number of samples selected from F . The direction of the edge is indicated by the position inside the concatenation. W denotes the weight matrix for the graph aggregation. If the weight matrix after random edge dropout is $W^* = Q^* \cdot W$, the final output for clip i can be obtained as

$$f_i^* = P_\theta \left(\sum_{j \in [0, N_s-1]} (r_{(i,j)} W_{(i,j)}^* f_j) \right), \quad (4)$$

$$f_i^* := \delta(\{f_i^* \mid i \in [0, N_s - 1]\})_i, \quad (5)$$

where f_i^* denotes the aggregated clip feature for clip i . δ denotes the bi-directional RNN with Long Short-Term Memory (LSTM) [23] as the cell for the temporal aggregation. P_θ denotes a linear projection layer. N_s denotes the total number of clips selected for input. We take the last clip after the temporal causal aggregation as the aggregated clip features $f^a = f_{N_s-1}^*$ for the final classification.

ASE Loss. The labels of the source domain and the target domain are identical. Motivated by this, we leverage the semantic embedding space of a pre-trained language model denoted as $\Phi(\cdot)$, *e.g.*, BERT [14], as an intermediate bridge between two domains. Let

B represent a batch of the labeled source and target samples with its label set L_B . Then, we can obtain the fully-connected adjacency matrix Adj_s according to the extracted semantic embedding as Eq. 6,

$$Adj_s = \{d_{\cos}(\Phi(s_x), \Phi(s_y)) \mid x \in L_B, y \in L_B\}, \quad (6)$$

where s_x indicates the context description for the x -th label in the batch and $d_{\cos}(\cdot)$ denotes the cosine distance. Similarly, the adjacency matrix of the samples on the video embedding space Adj_v in the corresponding selected batch could be derived as Eq. 7,

$$Adj_v = \{d_{\cos}(f_x^a, f_y^a) \mid x \in L_B, y \in L_B\}. \quad (7)$$

After the acquisition of the adjacency matrix in both the semantic embedding space and the video embedding space, the ASE loss is thereby calculated as Eq. 8,

$$L_{ASE} = d_{mse}(Adj_s, Adj_v), \quad (8)$$

where $d_{mse}(\cdot)$ denotes the mean squared error loss. The ASE loss encourages the embedding in the video latent space to have the same distance of the embedding in the semantic space considering all the different classes, which could be used even if the dimension of the semantic embedding does not match the dimension of the video embedding. Both samples from the training sets of the source and target domains are constrained by the ASE loss to use the semantic embedding space as a bridge between the two domains.

DPS Loss. To more effectively utilize the critical guidance for domain adaptation (DA) offered by the limited few-shot labeled samples from the target domain, we compute epoch-specific prototypes for each class within the target domain. We then encourage the embeddings from the source domain to align closely with the corresponding prototype embeddings in the target domain. As a result, we refer to this loss function as Domain Prototypical Similarity (DPS) loss. Let us define the set of prototypes as P , the target domain’s label set as L_t , and the unique label set as L_u . Given these definitions, the update process can be represented as follows in Eq. 9:

$$P = \{p_c \mid c \in L_u\}, \text{ where } p_c = \sum_m (f_{(m,c)}^a) / N_c, \quad (9)$$

where c is the class index, m is the sample index inside class c , p_c indicates the prototype of class c from the target domain and N_c indicates the sample number inside class c . Assuming a batch of the source-domain samples as S with labels L_S , the corresponding prototypes could be selected according to the labels of the source domain data and denoted as P_S , the DPS loss is calculated by Eq. 10,

$$L_{DPS} = \sum_{z \in [0, N_I - 1]} d_{\cos}(f_z^a, p_z) / N_I, \text{ where } p_z \in P_S, \quad (10)$$

where N_I indicates the sample number in the source domain training set per batch, z is the sample index, and L_{DPS} indicates the DPS loss.

Final loss. Apart from the aforementioned DPS loss and the ASE loss, cross-entropy-based classification loss L_{CLS} is used for the samples from both domains. All the losses are weighted and summed together while the weighted parameters are achieved by grid search. The final loss function can be calculated as Eq. 11,

$$L_{final} = w_1 * L_{DPS} + w_2 * L_{ASE} + w_3 * L_{CLS}. \quad (11)$$

4 EXPERIMENTS

4.1 Datasets

We utilize five popular human activity recognition datasets, *e.g.*, HMDB-51 [32], UCF-101 [53], EPIC-KITCHENS-55 [12], Toyota Smart Home (TSH) [13], and Sims4Action [48], to investigate FSDA-AR. The selected datasets comprise diverse activities and recording environments, enabling comprehensive evaluation of DA techniques. **HMDB-51** [32] contains 6,766 video clips from various sources, spanning across 51 activities categories with a minimum of 101 clips per activity. **UCF-101** [53] consists of 13,320 video clips, divided into 101 activity categories. These datasets are employed in the HMDB \rightarrow UCF and UCF \rightarrow HMDB adaptation tasks where they share 12 classes. **EPIC-KITCHENS-55** [12] comprises 55 hours of egocentric videos, capturing kitchen activities performed by 32 participants, and is utilized in the Epic-Kitchens domain adaptation task. We make use of the domain adaptation benchmark defined by [44] on 8 overlapped activities. **Toyota Smart Home** (TSH) [13] includes 16,115 video clips, containing 31 daily living activities. **Sims4Action** [48] is a synthetic dataset that was specifically designed for cross-domain evaluation on TSH. It comprises 13,232 video clips, depicting 10 daily living activities performed by avatars in the Sims 4 game, these datasets are used in the Sims4Action \rightarrow TSH adaptation task. These datasets serve as a robust foundation for exploring DA techniques in various cross-domain scenarios, offering challenges inherent in real-world and synthetic video data.

4.2 Implementation details

We randomly select N_{shot} samples per class on the training set of the target domain to construct our benchmarks, where $N_{shot} \in \{1, 5, 10, 20\}$. The few-shot samples are fixed to achieve better knowledge guidance through the co-training between the source and target domains. In order to make a fair comparison, all the feature extraction backbone is unified as I3D [3] initialized with Kinetics400 [30] pre-trained weight. Our model is trained on NVIDIA-A100 using PyTorch 1.12 with batch size 32, step-wise learning rate decay at epoch 60 and 80, the Adam [31] optimizer and initial learning rate 0.0001 for 100 epochs. The sliding window size for the feature extraction is set as 16 while temporal zero padding 8 is used. The dimension of the video-based latent space is chosen as 1024 while the dimension of the BERT [14] semantic feature is 768. All the hyperparameters of our FeatFSDA model are selected through grid search and provided in the supplementary.

4.3 Analysis of the benchmark

The results on our UCF [53] \rightarrow HMDB [32], HMDB [32] \rightarrow UCF [53], EPIC-KITCHEN [12], Sims4Action [48] \rightarrow TSH [13] benchmarks are provided in Table 1 (1, 2 and 3) and Table 2b, respectively. Both, UDA methods (implemented in FSDA-AR task) and existing published FSDA-AR methods show good performance and surpass Random obviously, which showcases that the domain gap can be reduced using fewer labeled shots, however, the required sample number is reduced largely, *e.g.*, for the five shots setting, the total required sample number is only around 2% of the sample number used in UDA setting. We notice that the performance of the TransVAE [62] is worse on FSDA-AR task while its performance

Methods	Shot-1	Shot-5	Shot-10	Shot-20	Shot-1	Shot-5	Shot-10	Shot-20	Shot-1	Shot-5	Shot-10	Shot-20	
	① UCF → HMDB				② HMDB → UCF				③ EPIC-KITCHEN mean				
DG	Random	8.6				8.1				12.5			
	KNN	81.1				88.3				28.1			
	Nearest Center	83.9				91.5				27.4			
	Nearest Neighbor	80.1				88.6				25.5			
	S I3D [3]	77.5				88.8				35.3			
FSDA-AR	CoMix [49]	83.1	88.1	89.7	90.8	91.0	93.2	96.8	96.3	31.2	31.8	32.1	32.7
	CO ² A [11]	83.9	88.1	89.1	91.1	92.5	94.0	96.7	97.5	32.6	36.4	38.0	38.2
	TA ³ N [7, 8]	83.3	88.9	88.3	91.7	93.7	95.1	97.5	98.0	38.9	41.8	42.1	43.0
	TranSVAE [62]	82.3	82.8	83.2	84.8	89.7	89.0	94.4	95.1	37.6	41.1	40.8	43.3
	FS-ADA [38]	82.7	87.2	88.6	87.2	91.9	94.4	93.7	96.5	37.0	39.7	39.3	40.4
	PASTN [20]	83.4	86.2	88.3	89.8	91.2	94.2	95.8	96.5	36.1	40.5	40.3	42.5
	FeatFSDA (ours)	84.4	89.7	90.3	92.8	95.6	96.5	97.7	98.2	41.0	44.4	44.5	45.1

Table 1: FSDA-AR results on UCF [53] → HMDB [32], HMDB [32] → UCF [53] and EPIC-KITCHEN [12].

Methods	① D1 → D2				② D2 → D1				③ D1 → D3				
	S-1	S-5	S-10	S-20	S-1	S-5	S-10	S-20	S-1	S-5	S-10	S-20	
DG	Random	12.5				12.3				12.7			
	KNN	25.5				26.9				26.2			
	Nearest Center	24.0				29.2				29.2			
	Nearest Neighbor	22.1				24.9				26.6			
	S I3D [3]	32.8				35.4				34.1			
	FSDA-AR	CoMix [49]	31.5	32.0	34.3	35.7	25.2	27.9	31.1	29.9	30.0	30.4	28.5
CO ² A [11]		31.7	33.5	33.6	33.3	32.6	38.4	36.1	39.8	30.2	36.4	38.3	38.0
TA ³ N [7, 8]		36.8	39.0	40.2	43.5	36.8	42.6	40.4	40.5	36.7	40.2	41.0	40.3
TranSVAE [62]		32.9	39.5	39.5	42.8	35.3	40.4	37.5	41.7	37.0	39.1	40.3	42.3
FS-ADA [38]		36.4	38.1	38.4	37.7	34.7	36.8	39.1	39.3	36.1	37.4	38.2	40.5
PASTN [20]		33.3	38.2	37.7	41.3	34.0	38.9	36.8	40.9	35.3	39.4	39.0	41.0
FeatSFDA (ours)		38.3	44.0	42.9	44.8	38.4	43.7	42.3	43.9	38.4	42.1	41.7	43.5
Methods	④ D3 → D1				⑤ D2 → D3				⑥ D3 → D2				
	S-1	S-5	S-10	S-20	S-1	S-5	S-10	S-20	S-1	S-5	S-10	S-20	
DG	Random	12.6				12.3				12.4			
	KNN	27.4				28.5				33.9			
	Nearest Center	25.1				34.0				23.1			
	Nearest Neighbor	26.4				24.1				28.7			
	S I3D [3]	34.6				39.1				35.8			
	FSDA-AR	CoMix [49]	30.4	30.2	28.8	30.4	34.0	34.5	35.3	34.4	36.0	35.7	34.5
CO ² A [11]		34.0	36.6	40.5	40.0	34.7	36.6	40.5	40.0	32.6	36.8	39.0	38.6
TA ³ N [7, 8]		39.1	40.0	40.9	41.8	41.1	43.4	43.5	45.6	42.8	45.8	46.5	46.5
TranSVAE [62]		36.1	38.2	37.5	41.4	42.8	44.9	44.5	45.9	41.2	44.4	45.6	45.6
FS-ADA [38]		32.2	39.8	35.9	38.6	42.4	42.5	42.0	44.3	40.4	43.5	42.1	42.2
PASTN [20]		33.6	37.9	38.2	41.1	39.2	43.1	44.4	44.6	43.0	45.5	45.9	45.8
FeatSFDA (ours)		39.5	41.6	43.4	42.3	45.3	46.0	48.2	48.4	45.9	49.1	48.4	47.9

(a) Experimental results for each split for FSDA-AR on EPIC-KITCHEN [12] dataset.

Table 2: FSDA-AR results on each split of the EPIC-KITCHEN, Sims4Action [48] → TSH [13] and the ablations.

is better than TA³N [7, 8] on UDA task as reported in Table 3, indicating that disentanglement method on domain adaptation relies on large scale training data from the target domain to grasp the adaptation cues. Similar results can be found for the CoMix [49] approach, which relies on diverse backgrounds of the target domain to achieve the adaptation, especially considering the datasets with large domain gaps. We leverage the I3D [3] backbone in all our experiments to

ensure fair comparisons. *S I3D* indicates directly using I3D trained on the source domain for the testing of the target domain.

Yet, the existing approaches do not well use the labeled target domain samples as additional guidance. To delve into it, we leverage semantic embedding space as a bridge between the source and target domains by using ASE loss, the target-domain prototypes by using the DPS loss and the RGA-ED to bring more generalizability.

Methods	Shot-1	Shot-5	Shot-10	Shot-20	
DG	Random	11.1			
	KNN	3.3			
	Nearest Center	28.0			
	Nearest Neighbor	3.27			
	S I3D [3]	22.8			
FSDA-AR	CoMix [49]	24.2	20.6	28.9	35.5
	CO ² A [11]	21.9	26.6	34.0	42.1
	TA ³ N [7, 8]	21.1	29.8	35.8	42.7
	TranSVAE [62]	22.6	22.7	18.9	22.7
	FS-ADA [38]	17.1	22.6	28.3	28.0
PASTN [20]	22.6	22.6	22.6	22.6	
FeatFSDA (ours)	24.6	31.4	36.7	45.7	

(b) Experimental results for few-shot domain adaptation of Sims4Action [48] → TSH [13].

RGA-ED	ASE	DPS	Shot-1	Shot-5	Shot-10	Shot-20
			34.7	35.6	37.7	37.7
✓			35.1	37.8	38.1	39.7
✓	✓		36.7	42.0	39.5	41.3
✓	✓	✓	38.3	44.0	42.9	44.8

(c) Ablation study of the FeatFSDA components on EPIC-KITCHEN [12] D1 → D2.

Methods	Shot-1	Shot-5	Shot-10	Shot-20
① Ablation of the DPS loss.				
Source + Target DPS	33.7	40.0	42.4	43.3
Source DPS	33.1	40.3	42.5	43.2
Target DPS	38.3	44.0	42.9	44.8
② Ablation of the RGA-ED module.				
RNN	35.6	35.9	38.4	42.3
GA-ED	33.2	41.5	39.3	42.4
RGA	34.4	40.7	40.6	43.1
RGA-ND	32.7	41.1	40.1	44.3
RGA-ED	38.3	44.0	42.9	44.8

(d) Ablation of the DPS loss and RGA-ED on the EPIC-KITCHEN [12] D1 → D2.

Methods	Shot-1	Shot-5	Shot-10	Shot-20
1 UDA approaches on UDA task on EPIC-KITCHEN.				
TranSVAE [62]		52.6		
CoMix [49]		43.2		
TA ³ N [7, 8]		39.9		
DANN [19]		39.2		
ADDA [58]		39.2		
2 TA³N and FeatFSDA on FSDA-AR task on EPIC-KITCHEN.				
TA ³ N [7, 8]	38.9	41.8	42.1	43.0
FeatFSDA (ours)	41.0	44.4	44.5	45.1
3 UDA approaches for UDA tasks on UCF → HMDB.				
TranSVAE [62]		87.8		
CoMix [49]		86.7		
TA ³ N [7, 8]		81.4		
DANN [19]		80.1		
ADDA [58]		79.2		
4 TA³N and FeatFSDA for FSDA-AR task on UCF → HMDB.				
TA ³ N [7, 8]	83.3	88.9	88.3	91.7
FeatFSDA (ours)	84.4	89.7	90.3	92.8
5 UDA approaches for UDA tasks on HMDB → UCF.				
TranSVAE [62]		99.0		
CoMix [49]		93.9		
TA ³ N [7, 8]		90.5		
DANN [19]		88.1		
ADDA [58]		88.4		
6 TA³N and FeatFSDA for FSDA-AR task on HMDB → UCF.				
TA ³ N [7, 8]	93.7	95.1	97.5	98.0
FeatFSDA (ours)	95.6	96.5	97.7	98.2
7 UDA approaches for UDA task on Sims4Action → TSH.				
Schneider <i>et al.</i> [51]		36.3		
TA ³ N [7, 8] ([51])		8.0		
8 TA³N and FeatFSDA for FSDA-AR task on Sims4Action → TSH.				
TA ³ N [7, 8]	21.1	29.8	35.8	42.7
FeatFSDA (ours)	24.6	31.4	36.7	45.7

Table 3: Task comparison between the FSDA-AR and the UDA.

Comparing against the best baseline for each shot-setting, our proposed FeatFSDA achieves 2.1%, 2.6%, 2.4%, and 1.8% performance improvement for 1-, 5-, 10-, and 20-shot setting on EPIC-KITCHEN for FSDA-AR in Table 1 5. The per-split performances are shown in Table 2a, where FeatFSDA shows consistent superior results on the FSDA-AR task for each split of EPIC-KITCHEN [12]. Some UDA approaches implemented into FSDA-AR do not show better performances compared with *S3D* [3] indicating that fewer target domain samples may cause overfitting to some approaches on the datasets with large domain differences, *e.g.*, CoMix [49] on EPIC-KITCHEN [12], while FeatFSDA outperforms *S3D* overall.

Regarding the FSDA-AR task on the UCF [53] → HMDB [32] and HMDB [32] → UCF [53] introduced in Table 1 1 and 2, FSDA-AR benchmarks show promising performance even under 1-shot. CoMix [49], CO²A [11], and TA³N [7, 8] under FSDA-AR are better than the state-of-the-art performance 87.8% for UDA as in Table 3 1 when $N_{shot} \geq 5$ on the UCF [53] → HMDB [32], which demonstrates that FSDA-AR is more efficient compared with



Figure 3: Qualitative results for the FSDA-AR on Sims4Action [48] → TSH [13].

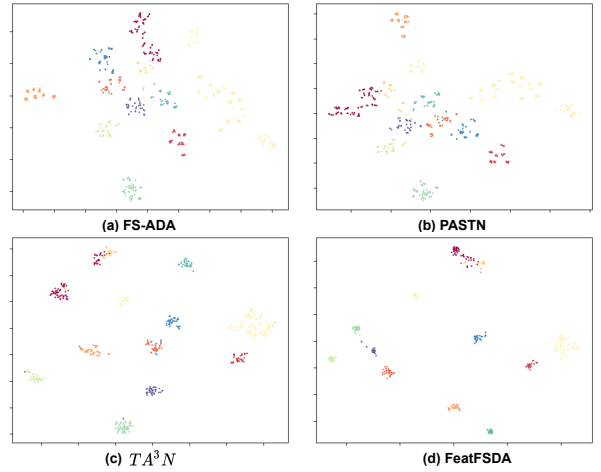


Figure 4: The t-SNE [59] visualization of the feature on the UCF [53] test set for FSDA-AR on HMDB [32] → UCF [53].

UDA under small domain gap. Compared with the approach with the best performance in all baselines for 1-20 shot settings, FeatFSDA achieves performance improvements with 0.5%, 0.8%, 0.6%, and 1.1% for FSDA-AR on the UCF [53] → HMDB [32] and 1.9%, 1.4%, 0.2%, and 0.2% on the HMDB [32] → UCF [53], respectively. Similar consistent performance improvement could also be found on the Sims4Action [48] → TSH [13]. Compared with the approach with the best performance in all the leveraged baselines for 1-20 shot settings, FeatFSDA achieves performance improvements with 0.4%, 1.6%, 0.9%, and 3.0% on Sims4Action [48] → TSH [13] as introduced in Table 2b. The consistent performance enhancements demonstrated by FeatFSDA across various datasets indicate that the three proposed components, such as ASE loss, DPS loss, and RGA-ED, effectively utilize the guidance provided by the few-labeled samples from the target domain. Furthermore, they achieve a generalizable temporal aggregation that accounts for diverse domain differences. In terms of video-based domain adaptation, the FSDA-AR task exhibits comparable performance to the UDA task for human activity recognition. Consequently, our experiments confirm the feasibility of FSDA-AR

and we believe it to be an essential future research direction in domain adaptation for human activity recognition.

4.4 Analysis of the ablations

Ablation of the individual building blocks. To validate the effectiveness of each proposed component, we perform ablation experiments on the EPIC-KITCHEN [12] D1-D2 split (Table 2c). When comparing the original model without any of the proposed components, FeatFSDA with RGA-ED, FeatFSDA with ASE loss and RGA-ED, and FeatFSDA with all the three proposed techniques, we observe performance improvements of 0.4%, 2.0%, 3.6% for 1-shot setting, 2.2%, 6.4%, 8.4% for 5-shot setting, 0.4%, 1.8%, 5.2% for 10-shot setting and 2.0%, 3.6%, 7.1% for 20-shot setting respectively. The benefits brought by each proposed component show consistent progressively increased improvements even across the different shot settings, demonstrating the benefits of our design.

Ablation of the DPS loss. The ablation of the DPS loss is illustrated in Table 2d ①. We compare our domain DPS loss which uses prototypes from the target domain (target-domain DPS loss) with the DPS loss which uses the prototypes calculated in the source domain (source-domain DPS loss) and the source-target domain DPS loss. Regarding the source domain DPS loss, we calculate the epoch-wise prototypes considering all the samples in the source domain and force the embeddings in the target domain to be more similar to the prototype embeddings calculated in the source domain. In the case of source-target domain DPS loss, we calculate the embedding prototypes for both source and target domain samples, and we encourage the target domain sample embeddings to align with the source domain prototypes while simultaneously promoting similarity between the source domain sample embeddings and the target domain prototypes. Experimental results indicate that pushing the source domain embeddings to be more similar to the target domain prototypes is beneficial, as it trains the classifier on embeddings that better align with the target domain style.

Ablation of the RGA-ED approach. Our next area of investigation is the proposed RGA-ED mechanism with the results provided in Table 2d ②. We compare RGA-ED with RNN-based aggregation (RNN), graph attentive network based aggregation with edge dropout (GA-ED), RNN + graph attentive network based aggregation (RGA), RNN + graph attentive network based aggregation + node dropout (RGA-ND). Compared to RGA-ND, RGA-ED demonstrates a 5.6% Top-1 accuracy improvement for the 1-shot FSDA-AR, highlighting the advantages of edge dropout over node dropout. This superiority can be attributed to the fact that node dropout leads to discontinuity in temporal cues and results in information loss, whereas edge dropout effectively preserves this information. Compared with RGA, RGA-ED obtains a performance boost of 3.9% (1-shot), suggesting that incorporating edge dropout effectively enhances the model’s generalizability for temporal aggregation. Compared with GA-ED, RGA-ED has a performance improvement by 5.1% for 1-shot demonstrating the benefits by using an additional RNN after the graph-based temporal aggregation. Compared with RGA, it turns out that incorporating edge dropout into RGA is essential, otherwise, the RNN and graph attentive network together would negatively impact model generalizability through increased capacity.

4.5 Comparison between UDA and FSDA-AR

Table 3 compares the FSDA-AR task we explored with the more conventional UDA setting. Our benchmark contains activity recognition datasets with diverse variations. UCF [53] → HMDB [32] and HMDB [32] → UCF [53] contain fewer domain shifts where DA is easy to be addressed. EPIC-KITCHENS [12] delivers samples for ego-central views which makes the activity recognition harder since only a part of the human body is visible. Sims4Action [48] → TSH [13] uses the synthesized and the daily life activity recognition dataset with a large domain gap. FeatFSDA (Table 3 ① and ④) shows better performance under FSDA-AR setting compared with other established approaches on the Sims4Action [48] → TSH [13] and UCF [53] → HMDB [32] for ≤ 20 shots setting in Table 3 ③ and ⑦. While considering the HMDB [32] → UCF [53] and EPIC-KITCHEN [12], FeatFSDA (Table 3 ⑥ and ②) shows comparative performance compared with the listed UDA approaches under UDA task in Table 3 ① and ④. However, if we compare the two tasks on the same method leveraged among all these datasets for UDA, e.g., TA³N, TA³N under FSDA-AR outperforms TA³N under UDA considering all datasets under ≤ 20 shots setting, which demonstrates the advantages of the FSDA-AR task and means that FSDA-AR could be a good choice for video-based DA when the data collection in the target domain is time-consuming.

4.6 Analysis of the qualitative results

Apart from the quantitative analysis, we further investigate the qualitative results from the proposed FSDA-AR task. As shown in ①–⑥ in Figure 3, we visualize six results of activity recognition from the setting of Sims4Action → TSH, including *Walk*, *Sit down*, *Use tablet*, *Watch TV*, *Cook*, and *Use telephone*. For each sample, we compare the activity predictions from FS-ADA [38], TA³N [7, 8], and our FeatFSDA, respectively. In such a new few-shot domain adaptation setting, the FS-ADA method cannot generalize well from the source domain to the target domain, and it recognizes all six activities as *Read Book*. In ②, ③, and ④, TA³N cannot correctly recognize the activities from the target domain. Thanks to the proposed losses and the RGA-ED technique, our FeatFSDA can obtain much better generalization ability and yields more correct results when performing few-shot domain adaptation. The qualitative results are consistent with our assumption that the model can benefit from the proposed techniques, and obtain generalizable temporal aggregation as well.

4.7 Analysis of the t-SNE visualization

In order to investigate the performance of few-shot domain adaptation, the commonly-used t-SNE method is applied to visualize the feature maps from the latent space. As presented in Figure 4, from (a) to (d) are the t-SNE features distributions from FS-ADA, PASTN, TA³N, and our FeatFSDA. Under the setting of HMDB [32] → UCF [53], the samples shown in Figure 4 are selected from the test set of the UCF. As compared to the other methods, the features from our FeatFSDA are more distinguishable across different classes in the latent space of the target domain, showing a better generalization ability of FeatFSDA, which is crucial in FSDA-AR.

5 CONCLUSION

In this work, we look into the few-shot domain adaptation of spatiotemporal architectures for video-based activity recognition. We establish the large-scale FSDA-AR benchmark with five datasets incorporating a variety of real-world, egocentric, and synthetic video data. We put forward the FeatFSDA solution which features a latent space semantic adjacency loss, a domain prototypical similarity loss, and an RNN-based graph attentive network with an edge dropout technique. FeatFSDA achieves state-of-the-art performance on all few-shot domain-adaptive settings in human activity recognition.

REFERENCES

- [1] Gedas Bertasius, Heng Wang, and Lorenzo Torresani. 2021. Is Space-Time Attention All You Need for Video Understanding?. In *ICML*, Vol. Vol. 139. 813–824. <http://proceedings.mlr.press/v139/bertasius21a.html>
- [2] Jie Cao, Youquan Wang, Haicheng Tao, and Xiang Guo. 2022. Sensor-based Human Activity Recognition Using Graph LSTM and Multi-task Classification Model. *TOMCCAP* Vol. 18 (2022), 139:1–139:19. <https://doi.org/10.1145/CVPR.2019.00752>
- [3] João Carreira and Andrew Zisserman. 2017. Quo Vadis, Action Recognition? A New Model and the Kinetics Dataset. In *CVPR*. 4724–4733. <https://doi.org/10.1109/CVPR.2017.502>
- [4] Woong-Gi Chang, Tackgeun You, Seonguk Seo, Suha Kwak, and Bohyung Han. 2019. Domain-Specific Batch Normalization for Unsupervised Domain Adaptation. In *CVPR*. 7354–7362. <https://doi.org/10.1109/CVPR.2019.00753>
- [5] Youngjae Chang, Akhil Mathur, Anton Isopoussu, Junehwa Song, and Fahim Kawsar. 2020. A Systematic Study of Unsupervised Domain Adaptation for Robust Human-Activity Recognition. *IMWUT* Vol. 4 (2020), 39:1–39:30. <https://doi.org/10.1145/3380985>
- [6] Chaoqi Chen, Weiping Xie, Wenbing Huang, Yu Rong, Xinghao Ding, Yue Huang, Tingyang Xu, and Junzhou Huang. 2019. Progressive Feature Alignment for Unsupervised Domain Adaptation. In *CVPR*. 627–636. <https://doi.org/10.1109/CVPR.2019.00072>
- [7] Min-Hung Chen, Zsolt Kira, and Ghassan AlRegib. 2019. Temporal Attentive Alignment for Video Domain Adaptation. *CoRR* abs/1905.10861 (2019). <http://arxiv.org/abs/1905.10861>
- [8] Min-Hung Chen, Zsolt Kira, Ghassan Alregib, Jaekwon Yoo, Ruxin Chen, and Jian Zheng. 2019. Temporal Attentive Alignment for Large-Scale Video Domain Adaptation. In *ICCV*. 6320–6329. <https://doi.org/10.1109/ICCV.2019.00642>
- [9] Jinwoo Choi, Gaurav Sharma, Samuel Schuller, and Jia-Bin Huang. 2020. Shuffle and Attend: Video Domain Adaptation. In *ECCV*, Vol. 12357. 678–695. https://doi.org/10.1007/978-3-030-58610-2_40
- [10] Xin Cong, Bowen Yu, Tingwen Liu, Shiyao Cui, Hengzhu Tang, and Bin Wang. 2020. Inductive Unsupervised Domain Adaptation for Few-Shot Classification via Clustering. In *ECML PKDD*, Vol. Vol. 12458. 624–639. https://doi.org/10.1007/978-3-030-67661-2_37
- [11] Victor G. Turrissi da Costa, Giacomo Zara, Paolo Rota, Thiago Oliveira-Santos, Nicu Sebe, Vittorio Murino, and Elisa Ricci. 2022. Dual-Head Contrastive Domain Adaptation for Video Action Recognition. In *WACV*. 2234–2243. <https://doi.org/10.1109/WACV51458.2022.00229>
- [12] Dima Damen, Hazel Doughy, Giovanni Maria Farinella, Sanja Fidler, Antonino Furnari, Evangelos Kazakos, Davide Moltisanti, Jonathan Munro, Toby Perrett, Will Price, and Michael Wray. 2018. Scaling Egocentric Vision: The EPIC-KITCHENS Dataset. *CoRR* (2018). <http://arxiv.org/abs/1804.02748>
- [13] Srijan Das, Rui Dai, Michal Koperski, Luca Minciullo, Lorenzo Garattoni, François Brémond, and Gianpiero Francesca. 2019. Toyota Smarthome: Real-World Activities of Daily Living. In *ICCV*. 833–842. <https://doi.org/10.1109/ICCV.2019.00092>
- [14] Jacob Devlin, Ming-Wei Chang, Kenton Lee, and Kristina Toutanova. 2019. BERT: Pre-training of Deep Bidirectional Transformers for Language Understanding. In *NAACL-HLT*. 4171–4186. <https://doi.org/10.18653/v1/n19-1423>
- [15] Zhekai Du, Jingjing Li, Hongzu Su, Lei Zhu, and Ke Lu. 2021. Cross-Domain Gradient Discrepancy Minimization for Unsupervised Domain Adaptation. In *CVPR*. 3937–3946. <https://doi.org/10.1109/CVPR46437.2021.00393>
- [16] Haoqi Fan, Bo Xiong, Kartikeya Mangalam, Yanghao Li, Zhicheng Yan, Jitendra Malik, and Christoph Feichtenhofer. 2021. Multiscale Vision Transformers. In *ICCV*. 6804–6815. <https://doi.org/10.1109/ICCV48922.2021.00675>
- [17] Junsong Fan, Zhaoxiang Zhang, Tieniu Tan, Chunfeng Song, and Jun Xiao. 2020. CIAN: Cross-Image Affinity Net for Weakly Supervised Semantic Segmentation. In *AAAI*. 10762–10769. <https://ojs.aaai.org/index.php/AAAI/article/view/6705>
- [18] Christoph Feichtenhofer. 2020. X3D: Expanding Architectures for Efficient Video Recognition. In *CVPR*. 200–210. <https://doi.org/10.1109/CVPR42600.2020.00028>
- [19] Yaroslav Ganin and Victor S. Lempitsky. 2015. Unsupervised Domain Adaptation by Backpropagation. In *ICML*, Vol. 37. 1180–1189. <http://proceedings.mlr.press/v37/ganin15.html>
- [20] Zan Gao, Leming Guo, Weili Guan, An-An Liu, Tongwei Ren, and Shengyong Chen. 2021. A Pairwise Attentive Adversarial Spatiotemporal Network for Cross-Domain Few-Shot Action Recognition-R2. *TIP* 30 (2021), 767–782. <https://doi.org/10.1109/TIP.2020.3038372>
- [21] Zhiqiang Gao, Shufei Zhang, Kaizhu Huang, Qiufeng Wang, Rui Zhang, and Chaoliang Zhong. 2022. Certifying Better Robust Generalization for Unsupervised Domain Adaptation. In *ACMMM*. 2399–2410. <https://doi.org/10.1145/3503161.3548323>
- [22] Kaiming He, Xiangyu Zhang, Shaoqing Ren, and Jian Sun. 2015. Deep Residual Learning for Image Recognition. *CoRR* (2015). <http://arxiv.org/abs/1512.03385>
- [23] Sepp Hochreiter and Jürgen Schmidhuber. 1997. Long Short-Term Memory. *Neural Comput.* 9, 8 (1997), 1735–1780. <https://doi.org/10.1162/neco.1997.9.8.1735>
- [24] Shengqi Huang, Wanqi Yang, Lei Wang, Luping Zhou, and Ming Yang. 2021. Few-shot Unsupervised Domain Adaptation with Image-to-Class Sparse Similarity Encoding. In *ACMMM*. 677–685. <https://doi.org/10.1145/3474085.3475232>
- [25] Yi Huang, Xiaoshan Yang, Junyu Gao, Jitao Sang, and Changsheng Xu. 2021. Knowledge-driven Egocentric Multimodal Activity Recognition. *TOMCCAP* Vol. 16 (2021), 133:1–133:133. <https://doi.org/10.1145/3409332>
- [26] Yi Huang, Xiaoshan Yang, Ji Zhang, and Changsheng Xu. 2022. Relative Alignment Network for Source-Free Multimodal Video Domain Adaptation. In *ACMMM*. 1652–1660. <https://doi.org/10.1145/3503161.3548009>
- [27] Junchang Jiang, Ximei Wang, Mingsheng Long, and Jianmin Wang. 2020. Resource Efficient Domain Adaptation. In *ACMMM*. 2220–2228. <https://doi.org/10.1145/3394171.3413701>
- [28] Taotao Jing, Haifeng Xia, Jihun Hamm, and Zhengming Ding. 2023. Marginalized Augmented Few-Shot Domain Adaptation. *TNNLS* (2023), 1–11. <https://doi.org/10.1109/TNNLS.2023.3263176>
- [29] Guoliang Kang, Lu Jiang, Yi Yang, and Alexander G. Hauptmann. 2019. Contrastive Adaptation Network for Unsupervised Domain Adaptation. In *CVPR*. 4893–4902. <https://doi.org/10.1109/CVPR.2019.00503>
- [30] Will Kay, João Carreira, Karen Simonyan, Brian Zhang, Chloe Hillier, Sudheendra Vijayanarasimhan, Fabio Viola, Tim Green, Trevor Back, Paul Natsev, Mustafa Suleyman, and Andrew Zisserman. 2017. The Kinetics Human Action Video Dataset. *CoRR* (2017). <http://arxiv.org/abs/1705.06950>
- [31] Diederik P. Kingma and Jimmy Ba. 2015. Adam: A Method for Stochastic Optimization. In *ICLR*. <http://arxiv.org/abs/1412.6980>
- [32] Hildebrandt Kuehne, Hueihan Jhuang, Estíbaliz Garrote, Tomaso A. Poggio, and Thomas Serre. 2011. HMDB: A large video database for human motion recognition. In *ICCV*. 2556–2563. <https://doi.org/10.1109/ICCV.2011.6126543>
- [33] Chen-Yu Lee, Tanmay Batra, Mohammad Haris Baig, and Daniel Ulbricht. 2019. Sliced Wasserstein Discrepancy for Unsupervised Domain Adaptation. In *CVPR*. 10285–10295. <https://doi.org/10.1109/CVPR.2019.01053>
- [34] Jichang Li, Guanbin Li, Yemin Shi, and Yizhou Yu. 2021. Cross-Domain Adaptive Clustering for Semi-Supervised Domain Adaptation. In *CVPR*. 2505–2514. <https://doi.org/10.1109/CVPR46437.2021.00253>
- [35] Jinfeng Li, Weifeng Liu, Yicong Zhou, Jun Yu, Dapeng Tao, and Changsheng Xu. 2022. Domain-invariant Graph for Adaptive Semi-supervised Domain Adaptation. *TOMCCAP* Vol. 18 (2022), 72:1–72:18. <https://doi.org/10.1145/3487194>
- [36] Mengxue Li, Yiming Zhai, You-Wei Luo, Pengfei Ge, and Chuan-Xian Ren. 2020. Enhanced Transport Distance for Unsupervised Domain Adaptation. In *CVPR*. 13933–13941. <https://doi.org/10.1109/CVPR42600.2020.01395>
- [37] Shuang Li, Chi Harold Liu, Binhui Xie, Limin Su, Zhengming Ding, and Gao Huang. 2019. Joint Adversarial Domain Adaptation. In *ACMMM*. 729–737. <https://doi.org/10.1145/3343031.3351070>
- [38] Xinyu Li, Yuan He, J. Andrew Zhang, and Xiaojun Jing. 2021. Supervised Domain Adaptation for Few-Shot Radar-Based Human Activity Recognition. *IEEE Sensors Journal* 21, 22 (2021), 25880–25890. <https://doi.org/10.1109/JSEN.2021.3117942>
- [39] Ze Liu, Jia Ning, Yue Cao, Yixuan Wei, Zheng Zhang, Stephen Lin, and Han Hu. 2022. Video Swin Transformer. In *CVPR*. 3192–3201. <https://doi.org/10.1109/CVPR52688.2022.00320>
- [40] Mingsheng Long, Yue Cao, Jianmin Wang, and Michael I. Jordan. 2015. Learning Transferable Features with Deep Adaptation Networks. In *ICML*, Vol. 37. 97–105. <http://proceedings.mlr.press/v37/long15.html>
- [41] Mingsheng Long, Han Zhu, Jianmin Wang, and Michael I. Jordan. 2017. Deep Transfer Learning with Joint Adaptation Networks. In *ICML*, Vol. 70. 2208–2217. <http://proceedings.mlr.press/v70/long17a.html>
- [42] Jianming Lv, Kaijie Liu, and Shengfeng He. 2021. Differentiated Learning for Multi-Modal Domain Adaptation. In *ACMMM*. 1322–1330. <https://doi.org/10.1145/3474085.3475660>
- [43] Saeid Motiian, Quinn Jones, Seyed Mehdi Iranmanesh, and Gianfranco Doretto. 2017. Few-Shot Adversarial Domain Adaptation. In *NIPS*. 6670–6680. <https://proceedings.neurips.cc/paper/2017/hash/21c5bba1dd6aed9ab48c2b34c1af0adde-Abstract.html>

- [44] Jonathan Munro and Dima Damen. 2020. Multi-Modal Domain Adaptation for Fine-Grained Action Recognition. In *CVPR*. 119–129. <https://doi.org/10.1109/CVPR42600.2020.00020>
- [45] Felix Ott, David Rügamer, Lucas Heublein, Bernd Bischl, and Christopher Mutschler. 2022. Domain Adaptation for Time-Series Classification to Mitigate Covariate Shift. In *ACMMM*. 5934–5943. <https://doi.org/10.1145/3503161.3548167>
- [46] Kunyu Peng, Alina Roitberg, Kailun Yang, Jiaming Zhang, and Rainer Stiefel-hagen. 2022. TransDARC: Transformer-based Driver Activity Recognition with Latent Space Feature Calibration. In *IROS*. 278–285. <https://doi.org/10.1109/IROS47612.2022.9981445>
- [47] Can Qin, Lichen Wang, Qianqian Ma, Yu Yin, Huan Wang, and Yun Fu. 2021. Contradictory Structure Learning for Semi-supervised Domain Adaptation. In *SDM*. 576–584. <https://doi.org/10.1137/1.9781611976700.65>
- [48] Alina Roitberg, David Schneider, Aulia Djamal, Constantin Seibold, Simon Reiß, and Rainer Stiefel-hagen. 2021. Let’s Play for Action: Recognizing Activities of Daily Living by Learning from Life Simulation Video Games. In *IROS*. 8563–8569. <https://doi.org/10.1109/IROS51168.2021.9636381>
- [49] Aadarsh Sahoo, Rutav Shah, Rameswar Panda, Kate Saenko, and Abir Das. 2021. Contrast and Mix: Temporal Contrastive Video Domain Adaptation with Background Mixing. *CoRR* (2021). <https://arxiv.org/abs/2110.15128>
- [50] Kuniaki Saito, Donghyun Kim, Stan Sclaroff, Trevor Darrell, and Kate Saenko. 2019. Semi-Supervised Domain Adaptation via Minimax Entropy. In *ICCV*. 8049–8057. <https://doi.org/10.1109/ICCV.2019.00814>
- [51] David Schneider, M. Saquib Sarfraz, Alina Roitberg, and Rainer Stiefel-hagen. 2022. Pose-based Contrastive Learning for Domain Agnostic Activity Representations. In *CVPR*. 3432–3442. <https://doi.org/10.1109/CVPRW56347.2022.00387>
- [52] Karen Simonyan and Andrew Zisserman. 2014. Two-Stream Convolutional Networks for Action Recognition in Videos. In *NIPS*. 568–576.
- [53] Khurram Soomro, Amir Roshan Zamir, and Mubarak Shah. 2012. UCF101: A Dataset of 101 Human Actions Classes From Videos in The Wild. *CoRR* (2012). <http://arxiv.org/abs/1212.0402>
- [54] Yu Sun, Eric Tzeng, Trevor Darrell, and Alexei A. Efros. 2019. Unsupervised Domain Adaptation through Self-Supervision. *CoRR* abs/1909.11825 (2019). <arXiv:1909.11825> <http://arxiv.org/abs/1909.11825>
- [55] Christian Szegedy, Wei Liu, Yangqing Jia, Pierre Sermanet, Scott E. Reed, Dragomir Anguelov, Dumitru Erhan, Vincent Vanhoucke, and Andrew Rabinovich. 2014. Going Deeper with Convolutions. *CoRR* (2014). <http://arxiv.org/abs/1409.4842>
- [56] Takeshi Teshima, Issei Sato, and Masashi Sugiyama. 2020. Few-shot Domain Adaptation by Causal Mechanism Transfer. In *ICML*, Vol. 119. 9458–9469. <http://proceedings.mlr.press/v119/teshima20a.html>
- [57] Du Tran, Lubomir D. Bourdev, Rob Fergus, Lorenzo Torresani, and Manohar Paluri. 2015. Learning Spatiotemporal Features with 3D Convolutional Networks. In *ICCV*. 4489–4497. <https://doi.org/10.1109/ICCV.2015.510>
- [58] Eric Tzeng, Judy Hoffman, Kate Saenko, and Trevor Darrell. 2017. Adversarial Discriminative Domain Adaptation. In *CVPR*. 2962–2971. <https://doi.org/10.1109/CVPR.2017.316>
- [59] Laurens Van der Maaten and Geoffrey Hinton. 2008. Visualizing data using t-SNE. *Journal of Machine Learning Research* 9, 11 (2008).
- [60] Petar Velickovic, Guillem Cucurull, Arantxa Casanova, Adriana Romero, Pietro Liò, and Yoshua Bengio. 2018. Graph Attention Networks. In *ICLR*. <https://openreview.net/forum?id=rJXMpikCZ>
- [61] Limin Wang, Yuanjun Xiong, Zhe Wang, Yu Qiao, Dahua Lin, Xiaoou Tang, and Luc Van Gool. 2016. Temporal Segment Networks: Towards Good Practices for Deep Action Recognition. In *ECCV*, Vol. 9912. 20–36. https://doi.org/10.1007/978-3-319-46484-8_2
- [62] Pengfei Wei, Lingdong Kong, Xinghua Qu, Xiang Yin, Zhiqiang Xu, Jing Jiang, and Zejun Ma. 2022. Unsupervised Video Domain Adaptation: A Disentanglement Perspective. *CoRR* (2022). <https://doi.org/10.48550/arXiv.2208.07365>
- [63] Zachary Wharton, Ardhendu Behera, Yonghui Liu, and Nik Bessis. 2021. Coarse Temporal Attention Network (CTA-Net) for Driver’s Activity Recognition. In *WACV*. 1278–1288. <https://doi.org/10.1109/WACV48630.2021.00132>
- [64] Lei Wu, Hefei Ling, Yuxuan Shi, and Baiyan Zhang. 2022. Instance Correlation Graph for Unsupervised Domain Adaptation. *TOMCCAP* Vol. 18 (2022), 33:1–33:23. <https://doi.org/10.1145/3486251>
- [65] Ni Xiao and Lei Zhang. 2021. Dynamic Weighted Learning for Unsupervised Domain Adaptation. In *CVPR*. 15242–15251. <https://doi.org/10.1109/CVPR46437.2021.01499>
- [66] Saining Xie, Chen Sun, Jonathan Huang, Zhuowen Tu, and Kevin Murphy. 2018. Rethinking Spatiotemporal Feature Learning: Speed-Accuracy Trade-offs in Video Classification. In *ECCV*, Vol. Vol. 11219. 318–335. https://doi.org/10.1007/978-3-030-01267-0_19
- [67] Yuecong Xu, Jianfei Yang, Haozhi Cao, Keyu Wu, Min Wu, and Zhenghua Chen. 2022. Source-Free Video Domain Adaptation by Learning Temporal Consistency for Action Recognition. In *ECCV*, Vol. 13694. 147–164. https://doi.org/10.1007/978-3-031-19830-4_9
- [68] Yuecong Xu, Jianfei Yang, Yunjiao Zhou, Zhenghua Chen, Min Wu, and Xiaoli Li. 2023. Augmenting and Aligning Snippets for Few-Shot Video Domain Adaptation. *CoRR* abs/2303.10451 (2023). <https://doi.org/10.48550/arXiv.2303.10451> [arXiv:2303.10451](https://arxiv.org/abs/2303.10451)
- [69] Luyu Yang, Yan Wang, Mingfei Gao, Abhinav Shrivastava, Kilian Q. Weinberger, Wei-Lun Chao, and Ser-Nam Lim. 2021. Deep Co-Training with Task Decomposition for Semi-Supervised Domain Adaptation. In *ICCV*. 8886–8896. <https://doi.org/10.1109/ICCV48922.2021.00878>
- [70] Jeongbeon Yoon, Dahyun Kang, and Minsu Cho. 2022. Semi-supervised Domain Adaptation via Sample-to-Sample Self-Distillation. In *WACV*. 1686–1695. <https://doi.org/10.1109/WACV51458.2022.00175>
- [71] Hongchuan Yu, Mengqing Huang, and Jian Jun Zhang. 2023. Domain Adaptation Problem in Sketch Based Image Retrieval. *TOMCCAP* Vol. 19 (2023), 17 pages. <https://doi.org/10.1145/3565368>
- [72] Jiawen Zhang, Jiaqi Zhu, Yi Yang, Wandong Shi, Congcong Zhang, and Hongan Wang. 2021. Knowledge-Enhanced Domain Adaptation in Few-Shot Relation Classification. In *SIGKDD*. 2183–2191. <https://doi.org/10.1145/3447548.3467438>
- [73] Weiming Zhang, Yi Huang, Wanting Yu, Xiaoshan Yang, Wei Wang, and Jitao Sang. 2019. Multimodal Attribute and Feature Embedding for Activity Recognition. In *ACMMMAsia*. 44:1–44:7. <https://doi.org/10.1145/3338533.3366592>

6 DISCUSSION OF SOCIETAL IMPACTS AND LIMITATION

Societal Impacts. In this work, we first construct the few-shot domain adaptation for activity recognition benchmark to enable more future research since the benchmark of the published paper [20] is unfortunately unavailable. We constructed the FSDA-AR benchmarks on five established activity recognition datasets, *e.g.*, HMDB-51 [32], UCF-101 [53], EPIC-KITCHEN [12], Sims4Action [48] and Toyota Smart Home (TSH) [13]. We further proposed a new approach, *i.e.*, FeatFSDA, which shows state-of-the-art performances on the proposed benchmark. Through our experiments, we find that all the leveraged approaches show comparable performances on the FSDA-AR task compared with UDA for human activity recognition. Using very few yet labeled samples sometimes even show better performance compared with using a large-scale unlabeled training set from the target domain, which emphasizes a new solution in applications while dealing with the video-based domain adaptation for a small domain gap. Unlike pixel-wise annotation which is used for semantic segmentation tasks, less time is required for the labeling work of human activity recognition tasks. In this case, FSDA-AR will be piratically useful since it will reduce 70% to 98% training samples on the target domain. However, our method does have false

Setting	FSDA				UDA
	S-1	S-5	S-10	S-20	
UCF [53]→HMDB [32]	12	60	120	240	840
HMDB [32]→UCF [53]	12	60	120	240	1438
Sims4Action [48]→TSH [13]	10	50	100	200	8552
D1→D2 [12]	8	40	80	160	2495
D2→D1 [12]	8	40	80	160	1543
D2→D3 [12]	8	40	80	160	3897
D3→D2 [12]	8	40	80	160	2495
D1→D3 [12]	8	40	80	160	3897
D3→D1 [12]	8	40	80	160	1543

Table 4: Details regarding the sample number that is required for FSDA-AR and UDA under each setting.

Setting	N_s				w_2				w_3			
	S-1	S-5	S-10	S-20	S-1	S-5	S-10	S-20	S-1	S-5	S-10	S-20
UCF [53]→HMDB [32]	12	12	14	14	0.001	0.1	0.1	0.1	0.0001	0.1	0.1	0.1
HMDB [32]→UCF [53]	12	12	12	12	0.01	0.01	0.01	0.01	0.001	0.001	0.001	0.001
Sims4Action [48]→TSH [13]	12	12	5	12	0.1	0.1	0.001	0.1	0.1	0.0001	0.1	0.001
D1→D2 [12]	12	10	10	12	0.001	0.1	10	0.01	10	10	10	0.001
D2→D1 [12]	12	12	10	12	1	1	0.1	0.001	1	1	0.01	0.001
D2→D3 [12]	12	12	12	12	0.1	0.1	0.1	0.1	0.1	0.1	0.1	0.1
D3→D2 [12]	12	12	12	12	0.1	0.1	0.1	0.1	0.1	0.1	0.1	0.1
D1→D3 [12]	14	12	14	14	0.001	0.1	0.1	0.1	10	10	10	10
D3→D1 [12]	12	12	21	12	0.001	0.1	0.1	0.1	0.001	0.1	0.01	0.1

Table 5: Hyper parameter setting for FeatFSDA.

μ	S-1	S-5	S-10	S-20
0.9	35.5	41.7	41.8	43.3
0.8	38.3	44.0	42.9	44.8
0.7	35.9	40.3	42.0	43.2
0.6	32.1	39.5	42.8	42.0
0.5	34.7	40.5	42.7	41.2

Table 6: Ablation for the choice of μ on EPIC-KITCHEN D1→D2.

μ	S-1	S-5	S-10	S-20
Fully connected	34.3	38.3	38.0	42.9
Ours	38.3	44.0	42.9	44.8

Table 7: Ablation experiments regarding the graph structure of RGA-ED on EPIC-KITCHEN D1→D2.

predictions as illustrated in the qualitative analysis in the main paper, which means our model has the potential to give offensive predictions, misclassifications, and biased content which may cause false predictions resulting in a negative social impact.

Limitations. In order to make a fair comparison with the existing UDA approaches on the UDA task, we unified the feature extraction backbone of all the leveraged approaches as I3D [3] pre-trained on the Kinetics400 [30] dataset. However, there are also other existing frameworks that could serve as feature extractors which will be considered in future work. The performance of the FeatFSDA approach still has a large space for further improvement on the FSDA-AR benchmark and FeatFSDA may cause false predictions in the real-world application as shown in the qualitative analysis part in our main paper. We only tackle the FSDA-AR for RGB video. Multi-modality FSDA-AR is not involved in this work, which will be addressed in future work.

	Methods	Shot-1	Shot-5	Shot-10	Shot-20
TARGET		① UCF → HMDB			
	Nearest Center	58.1	80.0	88.6	86.4
	Nearest Neighbor	58.6	76.4	80.0	84.4
		② HMDB → UCF			
	Nearest Center	64.6	85.5	94.7	93.7
	Nearest Neighbor	64.6	84.8	88.1	94.9
		③ EPIC-KITCHEN mean			
	Nearest Center	16.4	29.9	31.5	32.0
	Nearest Neighbor	16.4	27.1	29.2	31.2
		④ Sims4Action → TSH			
	Nearest Center	16.7	20.8	26.6	32.6
	Nearest Neighbor	16.7	23.7	33.5	35.4
SOURCE		① UCF → HMDB			
	Nearest Center	————— 24.0 —————			
	Nearest Neighbor	————— 22.1 —————			
		② HMDB → UCF			
	Nearest Center	————— 29.2 —————			
	Nearest Neighbor	————— 24.9 —————			
		③ EPIC-KITCHEN mean			
	Nearest Center	————— 29.2 —————			
	Nearest Neighbor	————— 26.6 —————			
		④ Sims4Action → TSH			
	Nearest Center	————— 28.0 —————			
	Nearest Neighbor	————— 3.3 —————			

Table 8: More statistic results on UCF [53] → HMDB [32], HMDB [32] → UCF [53] and EPIC-KITCHEN [12].

7 MORE DETAILS REGARDING THE FSDA-AR BENCHMARK

In this subsection, we will introduce more details regarding the FSDA-AR benchmark. We present the required sample number to formulate the training set on the target domain separately for FSDA-AR and UDA tasks on all the leveraged DA settings in Table 4. Compared with UDA, FSDA-AR requires obviously less data on the target domain for training. Since the labeling work for activity

recognition is not pixel-wise annotation and each sample only needs one label, the data collection may need more time than labeling one sample. In that case, our training set on the target domain for 20-shot setting needs obviously less time compared with the UDA task on each DA setting. On Sims4Action \rightarrow TSH, 97.7% of the samples from the target domain for the training are discarded in FSDA-AR compared with UDA, while FSDA-AR delivers better performance. As claimed in our main paper, the performance of FSDA-AR has comparable performance with UDA, which indicates that FSDA-AR is a more efficient setting, especially when the data collection in the target domain is hard to execute. We point out that FSDA-AR is an important research direction in the future and our work will serve as an important test bed in this direction.

8 ABLATION REGARDING THE GRAPH ARCHITECTURE USED FOR RGA-ED

As mentioned in our main paper, the graph structure leveraged in the proposed RGA-ED mechanism is not a fully-connected graph. We make use of a temporal causal directional graph to construct our RGA-ED mechanism. In order to showcase the efficacy of our design, we compare RGA-ED with a fully connected graph with our method in Table 7. Compared with the RGA-ED with a fully connected graph, our approach has overall superior performance among all the shot settings on the EPIC-KITCHENS D1 \rightarrow D2 dataset, which indicates that temporal causality is important to be considered while dealing with temporal aggregation in our model.

9 HYPER PARAMETER SELECTION

We make use of grid searching to find out the best hyperparameter of our approach under each DA setting. The range of N_s is set as [5, 16] with step size 1, the range of w_2 and w_3 is set as [0.0001, 10] with step multiplication factor 10 while w_1 is fixed as 1 and the edge dropout rate is set as 0.8. We present the selected parameters in Table 5 to get the best performance of our FeatFSDA approach. In Table 6 we present the ablation regarding different μ on EPIC-KITCHEN D1 \rightarrow D2. We find that the best choice of the μ is 0.8, which means that 20% edges are randomly dropped out. According to the reported results in Table 5, an appropriate μ is essential to harvest the most benefits brought by the RGA-ED mechanism and $\mu = 0.8$ is a suggested choice. If μ is too large, RGA-ED preserve less generalizability since fewer edges are changed during the training, which may result in an unsatisfied performance. However, if μ is very low, the temporal continuity will be broken which may cause a decay of the FSDA-AR performance. Apart from the above-mentioned hyperparameters, we choose the spatial size of the input RGB video as 224×224 .

10 MORE STATISTIC BASELINES.

We further provide the results for Nearest Neighbor and Nearest Center approaches by using the provided few shot labeled samples in the target domain training set as the reference and using the samples from the target domain test set as the query, as shown in Table 8 under *TARGET* group. To facilitate the comparison between the few-shot target-domain-based methods and source-domain-based methods, we reshew the results of the corresponding methods which use source domain training set as reference under the *SOURCE* group.

All the provided methods are executed on the extracted features through I3D [3] backbone pre-trained on Kinetics400 [30]. Compared with the performance under *SOURCE* setting, both Nearest Center and Nearest Neighbor approaches show better performance under *TARGET* settings considering ≤ 20 shots. This finding demonstrates the fact that providing few labeled shots does bring benefits for the FSDA-AR task.